International Journal of Nanoelectronics and Materials
Volume 16, No. 2, April 2023 [313-324]

Annealing temperature effect on TeO_2 thin films for optical detection devices

Ghadeer A. Mohi[1], Suad M. Kadhim [1], Hiba H. Abdullah[1*]

[1]Laser and Optoelectronics Engineering department, University of Technology, Baghdad, Iraq

Received 2 September 2022, Revised 3 October 2022, Accepted 12 October 2022

ABSTRACT

Physical vapor deposition method was used for the preparation of nanostructured TeO_2. Different morphologies of TeO_2 are synthesized using a physical evaporation method with Te powder as the source material and quartz SiO_2 as the growth substrates. X-ray diffraction (XRD), scanning electron microscopy (SEM), atomic force microscopy (AFM), and ultraviolet-visible (UV–Vis) analyses are used to characterize the structural, morphological, and optical properties of the TeO_2 products obtained. By varying the annealing temperature, different morphology of TeO_2 structures is investigated. TeO_2 nanostructure progress is initiated by the crystallization of particles. Different temperatures have different effects on structures, which are discussed. The films as deposited nature was amorphous; crystallization occurred at a higher annealing temperature (175 ^oC). With an increase in annealing temperature, the TeO_2 films grain size increased. The research also points to the impact of post-deposition thermal annealing temperatures in excess of 100 °C in enhancing TeO_2 film characteristics.

Keywords: annealing temperatures; nanoparticles; TeO_2; thin films.

1. INTRODUCTION

Nanotechnology is the science of modifying matter on a molecular and atomic scale [1]. It is associated with characterizing, producing, designing, and structuring systems and devices by manipulating one or more of their dimensions to nanometers [2]. Although significant efforts have been made to create high-quality metal oxide nanostructures, there are still many difficulties in doing so. These difficulties include, but are not limited to, the inability to reliably control length, diameter, orientation, crystallization, density, and hierarchical assembly [3].

A thin film is a thin layer of material with a thickness ranging from fractions of a nanometer to several micrometers [4]. Some of the most common methods for preparing thin films of semiconductors include vacuum thermal evaporation [5], spray pyrolysis [6], sputtering [7], and sol gel [8]. The majority of these methods are expensive and require a lot of time as well as a lot of vacuum and precise formation conditions [8]. Physical vapor deposition (PVD) techniques [9] have been widely adopted for the deposition of thin films in a variety of industrial fields: coating applications, manufacturing of metals, biomedical applications, and the coating of optical or electrical components [10].

*Corresponding author: Hiba.h.abdullah@uotechnology.edu.iq

Tellurium oxide (TeO_2) is distinctive due to its special characteristics [11]. TeO_2 has attracted a lot of interest for applications in piezoelectric and electro-optic systems [12]. Because of their great optical homogeneity, photo-elastic characteristics, and high optical damage resistance, tellurium dioxide crystals (TeO_2) play a significant role in acousto-optical devices [13], [14]. TeO_2 has an approximate 3.3 eV direct band gap and a 2.9 eV indirect band gap [15], [16].

In this study, the thermal evaporation approach was used to deposit a TeO_2 nanofilm. In order to examine and research the structural and optical characteristics of the thin films, they were also annealed at various temperatures.

2. MATERIAL AND METHODS

A thermal evaporation technique was used to grow thin films of TeO_2 on a quartz SiO_2 substrate, keeping the vacuum in the chamber on the order of 10^{-5} (mbar) during film deposition. A molybdenum boat was used to vaporize the TeO_2 powder. For this purpose, a high degree of purity (99.99 percent) of TeO_2 powder (approximately one gram) was loaded, which was connected to the evacuated system. Before beginning the dispersion, the quartz pieces were washed and sterilized with 99 percent absolute ethanol to remove any contaminants. By passing a current through the electrodes, the boat was indirectly heated. After achieving a large vacuum in the vacuum chamber and completing the evaporation process, samples were left to cool before being removed for annealing. Finally, TeO_2 thin films were annealed in an electric furnace at temperatures of 100 ^oC, 125 ^oC, 150 ^oC, and 175 ^oC. The temperature of the furnace was raised (at a rate of 25°C/h). The structural, electrical, and optical properties of TeO_2 films were studied. The nanostructures were obtained on the quartz substrates, and their morphology was studied using a scanning electron microscope (SEM), while the structural information was obtained using an X-ray diffractometer. Atomic Force Microscopy (AFM) was used to investigate three-dimensional surface topographic imaging, including surface roughness, grain size, and step height.

3. RESULTS AND DISCUSSION

3.1 Structural and Morphological Analysis:-

3.1.1 X-Ray Diffraction (XRD)

TeO_2 films that were deposited on SiO_2 quartz substrates and then annealed at temperatures of 100 ^oC, 125 ^oC, 150 ^oC, and 175 ^oC are depicted in Figure 1. The patterns show diffraction peaks of around (21.8^o), (26.4^o), (30.1^o), (37.2^o), (48.47^o) and (55.19^o) that, respectively, correspond to the TeO_2 diffraction plans (101), (110), (102), (200), (212) and (114) crystalline planes matching with JCPDS card number (11-0693). It is evident from the four diffraction patterns that the (101) and (110) directions is the favored orientation growth direction and that peaks intensity increases with annealing temperature [17]. Another peak for the diffraction pattern (111), confirming the presence of Te matching the card number (00-052-0795), appeared at 40.2^o during annealing in the electric furnace. The increased grain size of TeO_2 films with rising temperature may be responsible for this result, this agrees with other research [18]. A polycrystalline structure appeared for all samples with the same phases. Annealing enhances the crystallinity of samples, Indicate a growing in crystalline size (C.S) calculated from The Scherrer's formula [19], and decrease in dislocation density (d) as shown from Table 1, were used to calculate structural properties.

$$D = \frac{K.\lambda}{\beta.\cos\theta} \quad (1)$$

Where K is a constant value of 0.94, λ is the x-ray wavelength, Å, β is FWHM (full width at half maximum), and θ is the Bragg diffraction angle of the XRD peak (degree).

Table 1: X-ray different parameters of TeO_2 thin films.

Temp.(°C)	2θ (deg)	FWHM (deg)	d (Å)	C.S (nm)	hkl	Card no.
100 (°C)	21.6	1.094	4.298	7.454005	101	JCPDS 11-0693
	26.2	0.894	3.829	9.044468	110	
	30	0.578	3.012	13.87369	102	
	37.3	0.643	2.356	12.23343	200	
	48.4	0.623	1.945	12.15532	212	
	55.2	1.094	1.629	6.725618	114	
125 (°C)	21.69	0.1476	3.8172	55.24024	101	
	26.5	0.544	3.2074	14.85442	110	
	30	0.566	2.456	14.16783	102	
	37.4	0.673	2.2168	11.68466	200	
	48.45	0.984	1.9233	7.69439	212	
	55.4	1.094	1.45	6.719478	114	
150 (°C)	21.71	0.678	3.4375	12.02535	101	
	26.82	0.464	3.0318	17.40402	110	
	30.1	0.373	2.3319	21.49361	102	
	37.3	0.578	2.2265	13.60916	200	
	48.4	0.301	2.1015	25.15868	212	
	55.2	0.494	1.8424	14.89439	114	
175 (°C)	21.73	0.448	3.5359	18.19847	101	
	26.84	0.302	2.9371	26.73884	110	
	30.12	0.626	2.2341	12.80629	102	
	37.3	0.547	2.0613	14.38043	200	
	48.6	0.368	1.9304	20.56201	212	
	55.5	0.597	1.794	12.30778	114	

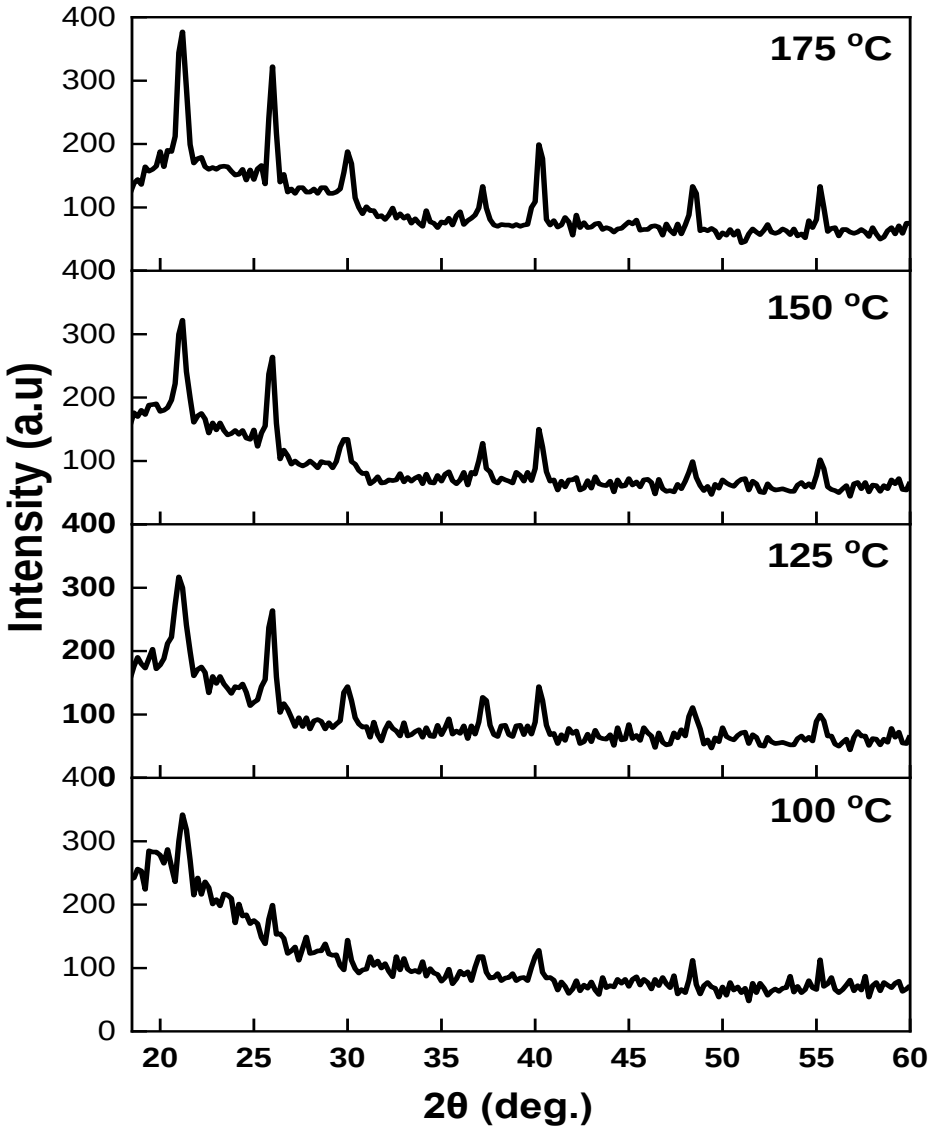

Figure 1:X-ray patterns of TeO_2 thin films for different annealing temperatures.

3.1.2 Atomic Force Microscope (AFM)

Figure 2 shows 2D and 3D AFM images of TeO_2 thin films deposited by PVD on SiO_2 quartz substrates and annealed at various temperatures. The surface structure of these films is clearly defined as the hierarchical shape of the grains appears at 100 °C and 125 °C and begins to decay as the annealing temperature rises to 175 °C. The average roughness of the nanostructures decreases as the annealing temperature increases, attributed to the atoms' ability to rearrange themselves with sufficient energy at a high deposition temperature to create a smooth surface [20]. Table 2 shows the calculated AFM parameters, which include mean roughness (Sa), mean root squared RMS (Sq) and mean grain size (D).

Table (2): AFM parameters

Temperature (°C)	Sa(nm)	Sq(nm)	D(nm)
100	2.9192	5.7214	10.24775552
125	2.3568	4.8356	16.39350399
150	1.6358	2.556	17.43086913
175	1.1951	1.7102	18.49897037

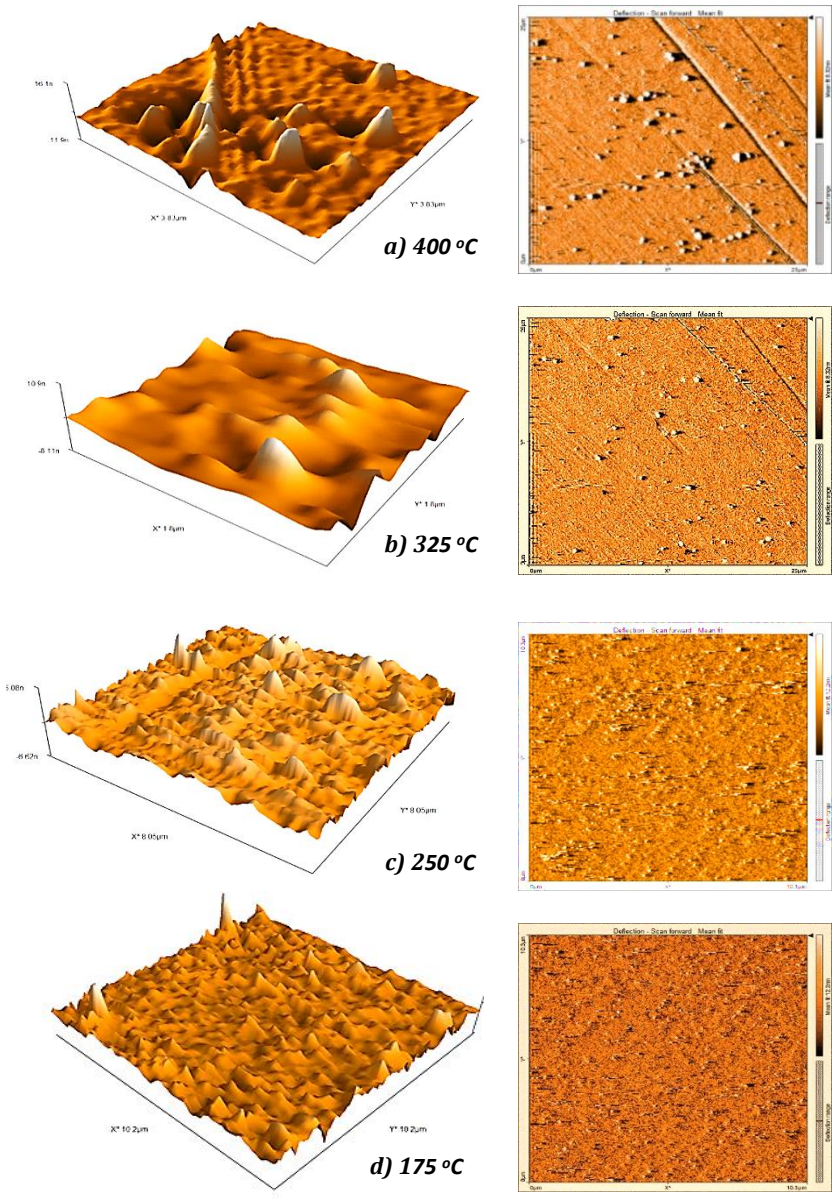

Figure 2: 2D and 3D AFM images of TeO_2 nanoparticles: a) 100 °C b) 125 °C c) 150 °C d) 175 °C.

3.1.3 Field Emission Scanning Electron Microscope (FE-SEM)

Figure 3 displays FE-SEM images of TeO2 thin films that were annealed at temperatures of 100 °C, 125 °C, 150 °C, and 175 °C. Almost all of the nanoparticles are visible independently or attached to the FE-SEM pictures, which demonstrate this. Using FE-SEM software, the grain diameter of the nanoparticles in samples with annealing temperatures of 125 °C, 150 °C, and 175 C was calculated to be between 35.13 and 82.65 nm, 40.4 to 66.2 nm, and 118.05 to 139.07 nm, respectively. After the samples were annealed, there was a noticeable rise in the size of the nanoparticles. Images demonstrate that the nanoparticles are amorphous and non-uniform, and that the grains become slightly crystalline as the annealing temperature is raised [21].

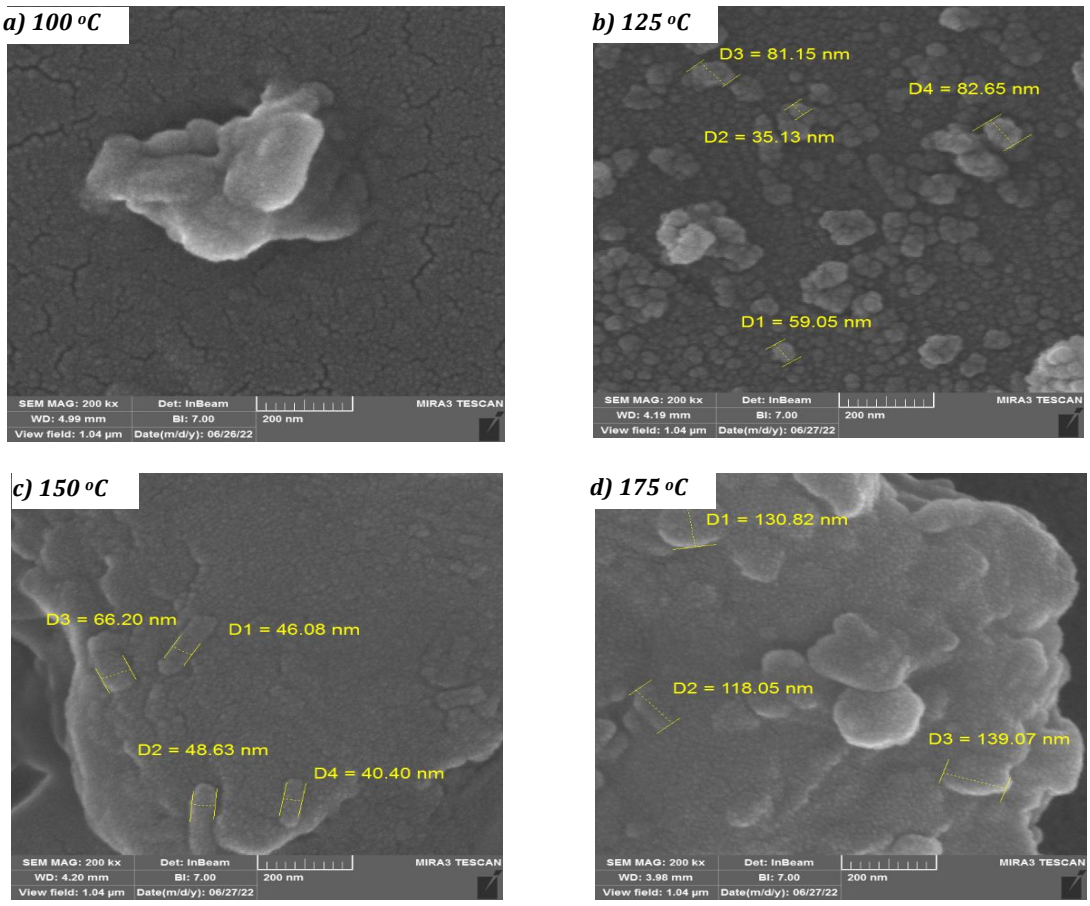

Figure 3: FE-SEM images of TeO2 thin films for different temperatures: a) 100 °C b) 125 °C c) 150 °C d) 175 °C.

3.2 Optical Properties:-

3.2.1 Transmission

The optical transmittance spectra of TeO_2 thin films at various temperatures are shown in Figure 4 with wavelengths ranging from 200 nm to 1100 nm. The results showed that the transmittance increases with increasing wavelength for all films. It is demonstrated that these films' transmission increases significantly between 380 and 410 nm.Moreover, it can be shown from these curves that the maximum transmittance of all thin films varies between 32.6% - 73.4%. The spectra indicate that the transmission has decreased as the temperature has increased from 100 ^oC to 175 ^oC, this is caused by an increase in the amount of light energy absorbed, which leads to an increase in the number of electronic transitions between the valence band and the conduction band [22].

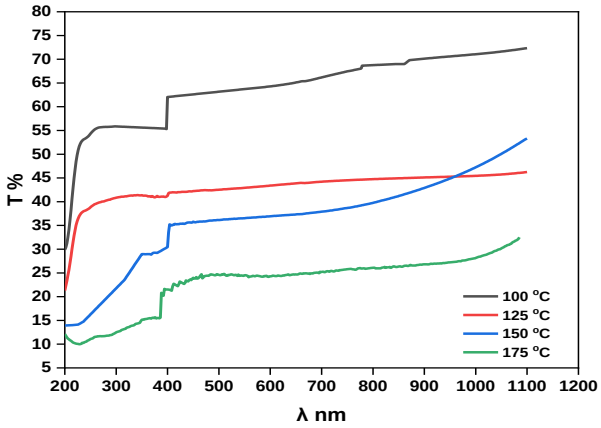

Figure 4: Optical transmittance spectra as a function of wavelength for TeO_2 with different annealing temperatures.

3.2.2 Absorbance

Under the same transmittance conditions, the absorbance measurements were investigated. The figure (5) depicts a plot of the absorbance graph as a function of wavelength.The results demonstrated that the absorbance of all deposited thin films decreases suddenly in the region of 380 nm to 410 nm, followed by a gradual decrease as wavelength increases. Moreover, as the annealing temperature rises, the absorbance rises as well, because larger crystalline sizes result in more atoms in the film increasing the number of states available for photons to be absorbed. The absence of oxygen and the presence of metallic Te could be one explanation for this absorption [23].

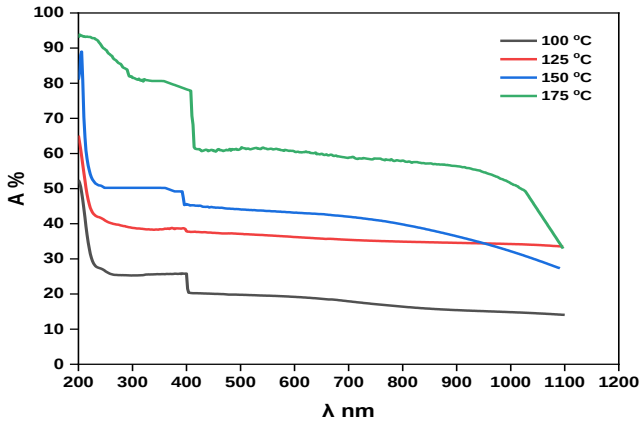

Figure 5: Optical Absorption spectra as a function of wavelength for TeO_2 with different annealing temperatures.

3.2.3 Absorption Coefficient

The values of the absorption coefficient for all tellurium oxide thin films were calculated using the following equation [24]:

$$\alpha = \frac{1}{d} ln \frac{1}{T} \quad (2)$$

Where d is the thickness of the thin film that has been deposited, and (T) is the transmission. A graphic correlation between the absorption coefficient and photon energy was established, as seen in Figure 6, we observe that for all films, the absorbance coefficient begins to increase as the annealing temperature increases. Additionally, absorption coefficient (α) gradually increases for all films with rising photon energy in the range of 1-2.8 eV, and then increases sharply over energies that are equal to or greater than the optical energy gap for all films in the range of 2.89-3.2 eV.

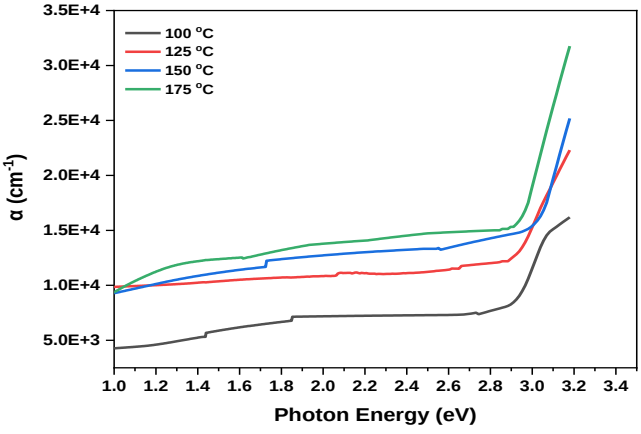

Figure 6: The absorption coefficient of TeO_2 thin films with different annealing temperatures.

3.2.4 Optical band gab:-

The energy gap provides a precise understanding of optical absorption since it shows that a film is transparent to radiation with energy below the energy gap (hυ ≤ Eg) but absorbs radiation with energy above it (hυ ≥ Eg). The following equation [25], [26] is used to calculate the energy gap Eg values of the tellurium oxide TeO_2 nanoparticles films:

$$\alpha h\upsilon = A(h\upsilon - Eg)^{0.5} \quad (3)$$

Where (A) is a constant, α is the absorption coefficient, υ is the photon frequency, and (h) is Planck's constant. It can be estimated using Tauc relation which depends on the graph of variables $(\alpha h\nu)^2$ in terms of (hν) as illustrated in Figure 7, the energy band gap measurements dropped from 3.145 eV to 2.892 eV as a result of an increase in annealing temperature. The individual levels of unbound atoms will widen the energy bands and produce overlapping levels. Atoms move toward one another, causing this. Because of this, these films' band gaps have multiple overlapping energy bands when the temperature increases. Therefore, the overlapping energy bands have a tendency to minimize the energy band gap, resulting in reduced band gaps with increases in annealing temperature; this is in good agreement with the previous studies [27].

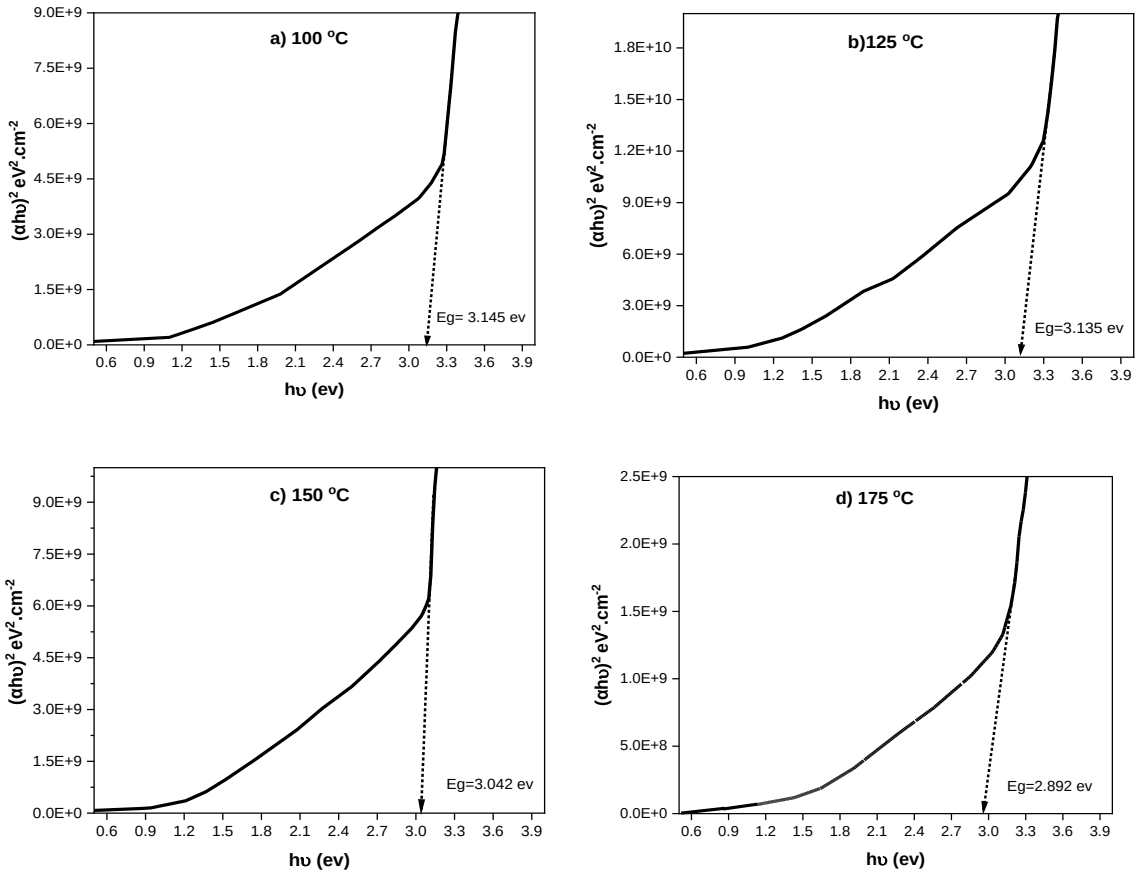

Figure 7: Variation of $(\alpha h\nu)^2$ with photon energy of TeO_2 thin films with different annealing temperatures.

4. CONCLUSION

In conclusion, Tellurium dioxide thin films with nanostructures were deposited using the thermal evaporation technique. The annealing procedure aids in enhancing the thin films' crystalline properties. According to (FE-SEM) and (AFM) analysis of all the films, the average diameter, average roughness, and RMS of the nanoparticle thin film increase with increasing the annealing temperature. The UV to the visible region of the Tellurium dioxide (UV-V) is spectrum of the nanoparticles exhibits the highest absorption. The analysis of the optical properties shows how effective the heat evaporation procedure is for depositing (TeO_2) thin films. The energy gap gradually narrows and the grain size steadily increases at the annealing temperatures of 100 ^oC and 125 ^oC. The energy gap significantly decreases and the particle size increases at temperatures between 150 ^oC and 175 ^oC under the same conditions as before.

ACKNOWLEDGEMENTS

The author is appreciative of the University of Technology-Iraq for its outstanding assistance.

Funding declaration

The study that was submitted by the authors was not funded by any organization.

Data availability statement

The author will provide the datasets created during the present research upon reasonable request.

REFERENCES

[1] E. Mostafavi, P. Soltantabar, and T. J. Webster, *Nanotechnology and picotechnology: A new arena for translational medicine*. Elsevier Inc., 2018. doi: 10.1016/B978-0-12-813477-1.00009-8.

[2] P. S. Mishra, H. Sharma, R. Mishra, and S. K. Gupta, "A REVIEW ON ANTI-MALARIAL DRUG DISCOVERY AND ITS," vol. 3, no. 8, pp. 1288–1304, 2014.

[3] T. Zhai *et al.*, "A comprehensive review of one-dimensional metal-oxide nanostructure photodetectors," *Sensors*, vol. 9, no. 8, pp. 6504–6529, 2009, doi: 10.3390/s90806504.

[4] M. Ohring, "The Materials Science of Thin Films Academic Press," *San Diego New yourk Bost.*, 1992.

[5] W. K. Khalef, "Nanostructure Cadmium Oxide Thin Film Prepared by Vacuum Evaporation Thermal Technique," *Eng. &Tech.Journal*, vol. 32, no. 5. pp. 1009–1018, 2014.

[6] K. O. Ukoba, A. C. Eloka-Eboka, and F. L. Inambao, "Review of nanostructured NiO thin film deposition using the spray pyrolysis technique," *Renew. Sustain. Energy Rev.*, vol. 82, no. July, pp. 2900–2915, 2018, doi: 10.1016/j.rser.2017.10.041.

[7] M. S. Bashar *et al.*, "Effect of rapid thermal annealing on structural and optical properties of ZnS thin films fabricated by RF magnetron sputtering technique," *J. Theor. Appl. Phys.*, vol. 14, no. 1, pp. 53–63, 2020, doi: 10.1007/s40094-019-00361-5.

[8] H. S. Ullal, K. Zwelbel, and B. Von Roedern, "Current status of polycrystalline thin-film PV

technologies," in *Conference Record of the Twenty Sixth IEEE Photovoltaic Specialists Conference-1997*, 1997, pp. 301–305.

[9] F. K. Challab* and S. K. J. , Maan A. Tawfiq, "Studying the Effect of un Coated and Multilayer Coated Tools on Cutting Temperature in Turning Operation." University of Technology-Iraq, pp. 66–75, 2022. doi: http://dx.doi.org/10.30684/etj.v40i6.2265.

[10] S. M. Rossnagel, "Thin film deposition with physical vapor deposition and related technologies," *J. Vac. Sci. Technol. A Vacuum, Surfaces, Film.*, vol. 21, no. 5, pp. S74–S87, 2003, doi: 10.1116/1.1600450.

[11] A. V. Vinogradov, V. A. Lomonov, Y. A. Pershin, and N. L. Sizova, "Growth and some properties of TeO2 single crystals with a large diameter," *Crystallogr. Reports*, vol. 47, no. 6, pp. 1036–1040, 2002, doi: 10.1134/1.1523523.

[12] P. S. Peercy, I. J. Fritz, and G. A. Samara, "Temperature and pressure dependences of the properties and phase transition in paratellurite (TeO2: Ultrasonic, dielectric and Raman and Brillouin scattering results," *J. Phys. Chem. Solids*, vol. 36, no. 10, pp. 1105–1122, 1975, doi: 10.1016/0022-3697(75)90053-0.

[13] S. Beke, K. Sugioka, K. Midorikawa, Á. Péter, L. Nánai, and J. Bonse, "Characterization of the ablation of TeO2 crystals in air with femtosecond laser pulses," *J. Phys. D. Appl. Phys.*, vol. 43, no. 2, 2010, doi: 10.1088/0022-3727/43/2/025401.

[14] N. Uchida and Y. Ohmachi, "Elastic and photoelastic properties of TeO2 single crystal," *J. Appl. Phys.*, vol. 40, no. 12, pp. 4692–4695, 1969, doi: 10.1063/1.1657275.

[15] T. Hesabizadeh *et al.*, "Synthesis of ' Naked ' TeO 2 Nanoparticles for Biomedical Applications," 2022, doi: 10.1021/acsomega.2c02316.

[16] S. Moufok, L. Kadi, B. Amrani, and K. D. Khodja, "Electronic structure and optical properties of TeO 2 polymorphs," *Results Phys.*, vol. 13, no. April, p. 102315, 2019, doi: 10.1016/j.rinp.2019.102315.

[17] T. Siciliano, M. Di Giulio, M. Tepore, E. Filippo, G. Micocci, and A. Tepore, "Effect of thermal annealing time on optical and structural properties of TeO2 thin films," *Vacuum*, vol. 84, no. 7, pp. 935–939, 2010, doi: 10.1016/j.vacuum.2009.12.017.

[18] A. Sudha, T. K. Maity, S. L. Sharma, and A. N. Gupta, "An extensive study on the structural evolution and gamma radiation stability of TeO2 thin films," *Mater. Sci. Semicond. Process.*, vol. 74, no. November 2017, pp. 347–351, 2018, doi: 10.1016/j.mssp.2017.10.018.

[19] S. Mustapha *et al.*, "Comparative study of crystallite size using Williamson-Hall and Debye-Scherrer plots for ZnO nanoparticles," *Adv. Nat. Sci. Nanosci. Nanotechnol.*, vol. 10, no. 4, 2019, doi: 10.1088/2043-6254/ab52f7.

[20] A. G. Kalampounias, G. Tsilomelekis, and S. Boghosian, "Glass-forming ability of TeO 2 and temperature induced changes on the structure of the glassy , supercooled , and molten states," vol. 154503, pp. 1–11, 2015.

[21] V. Adimule, R. G. Revaiah, S. S. Nandi, and A. H. Jagadeesha, "Synthesis, Characterization of Cr Doped TeO2 Nanostructures and its Application as EGFET pH Sensor," *Electroanalysis*, vol. 33, no. 3, pp. 579–590, 2021, doi: 10.1002/elan.202060329.

[22] R. Nayak, V. Gupta, A. L. Dawar, and K. Sreenivas, "Optical waveguiding in amorphous tellurium oxide thin films," *Thin Solid Films*, vol. 445, no. 1, pp. 118–126, 2003, doi: 10.1016/S0040-6090(03)01284-7.

[23] E. E. K. and J. S. M F Al-Kuhaili1, S MA Durrani2, "Effects of preparation conditions on the optical properties of thin films of tellurium oxide M," *Phys. D Appl. Phys.*, 2002, doi: https://doi.org/10.1088/0022-3727/35/9/312.

[24] C. A. H. M. A. HASSAN, "A study of the structural , electrical and optical properties of copper tellurium oxide glasses," *J. Mater. Sci.*, vol. 23, pp. 2500–2504, 1988.

[25] A. A. Aljubouri, A. D. Faisal, and W. K. Khalef, "Fabrication of temperature sensor based on copper oxide nanowires grown on titanium coated glass substrate," *Mater. Sci. Pol.*, vol. 36, no. 3, pp. 460–468, 2018, doi: 10.2478/msp-2018-0051.

[26] W. K. Khalef, T. R. Marzoog, and A. D. Faisal, "Synthesis and characterization of tellurium oxide nanoparticles using pulse laser ablation and study their antibacterial activity," *J.*

Phys. Conf. Ser., vol. 1795, no. 1, 2021, doi: 10.1088/1742-6596/1795/1/012049.

[27] A. Shirpay and M. M. B. Mohagheghi, "The effect of WO3/TeO2 molar concentration on the structural, optical, and thermoelectric properties of WO3–TeO2 binary thin films," *J. Mater. Sci. Mater. Electron.*, vol. 32, no. 2, pp. 1766–1777, 2021, doi: 10.1007/s10854-020-04944-w.